Carbohydrate Polymers 92 (2013) 1896–1900

Contents lists available at SciVerse ScienceDirect

Carbohydrate Polymers

journal homepage: www.elsevier.com/locate/carbpol

Arabinoxylan-mediated synthesis of gold and silver nanoparticles having exceptional high stability

Muhammad Amin[a], Fozia Iram[b], Mohammad S. Iqbal[c,*], Muhammad Z. Saeed[d], Mohsin Raza[a], Shehzad Alam[e]

[a] Department of Chemistry, University of Sargodha, Sargodha 40100, Pakistan
[b] Department of Chemistry, LCW University, Lahore 54600, Pakistan
[c] Department of Chemistry, Forman Christian College, Lahore 54600, Pakistan
[d] Department of Physics, COMSATS Institute of Information Technology, Park Road, Chak Shahzad, Islamabad, Pakistan
[e] Pakistan Council of Scientific and Industrial Research Laboratories Complex, Lahore 54600, Pakistan

ARTICLE INFO

Article history:
Received 27 October 2012
Received in revised form
10 November 2012
Accepted 21 November 2012
Available online 28 November 2012

Keywords:
Gold nanoparticles
Silver nanoparticles
Arabinoxylan
Green synthesis
Electron microscopy

ABSTRACT

A green synthesis of highly stable gold and silver nanoparticles (NPs) using arabinoxylan (AX) from ispaghula (*Plantago ovata*) seed husk is being reported. The NPs were synthesized by stirring a mixture of AX and $HAuCl_4 \cdot H_2O$ or $AgNO_3$, separately, below 100 °C for less than an hour, where AX worked as the reducing and the stabilizing agent. The synthesized NPs were characterized by surface plasmon resonance (SPR) spectroscopy, transmission electron microscopy (TEM), atomic force microscopy (AFM), and X-ray diffraction (XRD). The particle size was (silver: 5–20 nm and gold: 8–30 nm) found to be dependent on pH, temperature, reaction time and concentrations of AX and the metal salts used. The NPs were poly-dispersed with a narrow range. They were stable for more than two years time.

1. Introduction

Nanotechnology is a growing area of interest because of its versatile applications in the fields ranging from electronics to medicine (Du, Niu, Xu, Xu, & Fan, 2009; Mubarak, Thajuddin, Jeganathan, & Gunasekaran, 2011; Sun & Xia, 2003; Yan et al., 2006; You, Chompoosor, & Rotello, 2007). Gold and silver NPs find extensive use in medicine, catalysis and electronics. Several synthetic methods have been employed for their preparation. These include physical, chemical and biochemical techniques. Chemical methods involve the use of noxious reducing agents, like sodium borohydride (Van Hyning & Zukoski, 1998) and hydrazine (Guzmán, Dille, & Godet, 2009), and hazardous costly solvents. The particles produced by these methods usually are unstable and as such require a stabilizing agent to be included in the process of synthesis. With increasing awareness about environmental impact of synthetic methods, it is always desirable to use the so-called green chemistry approach. Therefore, methods have been developed where the additional use of reducing and stabilizing agents can be avoided (Kora, Sashidhar, & Arunachalam, 2010; Raveendran, Fu, & Wallen, 2003). For application of NPs in medicine it is more important that all the materials used as aids in synthesis should be biocompatible. Keeping in view these requirements we here have used AX isolated from ispaghula seed husk as the reducing and dispersing agent.

AXs are gel-forming food components that are not hydrolyzed by enzymes of the upper gastrointestinal tract, and coagulate at an acidic pH. Thus they can deliver the encapsulated material into the last part of the large intestine (colon). AXs from isphagula (*Plantago ovata*) seed husk are abundantly available and well-characterized materials with potential use as drug carriers (Akbar, Iqbal, Chaudhary, Yasin, & Massey, 2012; Saghir, Iqbal, Hussain, Koschella, & Heinze, 2008). The AXs are composed of reducing sugars which can reduce gold or silver ions to particles and at the same time, having a hydrogel-like network, can disperse the particles in themselves. They have also been proved to be non-toxic for drug delivery (Iqbal, Akbar, Hussain, Saghir, & Sher, 2011). Therefore, we report here, for the first time, the use of AX from ispaghula for green synthesis of gold and silver NPs having exceptional high stability, which may find their use in medicine.

* Corresponding author. Tel.: +92 300 4262813.
E-mail address: saeediq50@hotmail.com (M.S. Iqbal).

0144-8617/$ – see front matter © 2012 Elsevier Ltd. All rights reserved.
http://dx.doi.org/10.1016/j.carbpol.2012.11.056

Table 1
Sample codes, inputs of materials and particle size ranges.

Code	AX-Sus (mL)	1.0 mM $HAuCl_4 \cdot 3H_2O$ (mL)	1.0 mM $AgNO_3$ (mL)	Water (mL)	NP size range under optimum conditions from TEM (nm)	
					Gold	Silver
G1/S1	2	10	10	8	35–40	18–25
G2/S2	4	10	10	6	30–35	15–22
G3/S3	6	10	10	4	20–35	10–20
G4/S4	8	10	10	2	8–30	8–20
G5/S5	10	10	10	–	15–30	5–20
G6/S6	10	8	8	2	50–60	30–50

Note: G: gold; S: silver.

2. Experimental

2.1. Materials

$HAuCl_4 \cdot 3H_2O$, $AgNO_3$, NaOH and CH_3COOH were of analytical grade and procured from Sigma Aldrich Co., USA. Ispaghula (*P. ovata*) seed husk was obtained from local market. Nanopure® water was used in this work.

2.2. Isolation of AX

Ispaghula seed husk (5.0 g) was soaked in Nanopure® water (200 mL) for 24 h in a clean environment. The AX gel was filtered under vacuum by use of a muslin cloth, washed several times with Nanopure® water, and the suspension was reduced by evaporation under vacuum to 100 mL (AX-Sus) for use in synthesis of NPs. In order to determine the reproducibility three batches of AX-Sus were prepared from ispaghula seed husk obtained from three different sources. The isolated AX was characterized by sugar analysis, gel permeation chromatography and FT-IR spectroscopy, and found to be similar to that reported previously (Saghir et al., 2008).

2.3. Synthesis of NPs

To an appropriate amount of AX-Sus, prepared above, 10 mL of $HAuCl_4 \cdot 3H_2O$ solution (1.0 mM) was added dropwise under vigorous stirring by use of a magnetic stirrer-cum-hotplate at ambient to 100 °C. The inputs of the reagents used in the synthesis and the sample codes are given in Table 1. Reduction of Au^{3+} to Au^0 was evident from a color change (orange to purple), which was complete within 60 min time. The experiment was repeated by using 2.0 and 3.0 mM $HAuCl_4 \cdot 3H_2O$ separately in order to study the effect of concentration of the gold salt on NPs. The effect of time and pH was studied by changing time from 10 to 180 min and pH from 2 to 7 (for gold) and 4 to 10 (for silver). The SPR spectra of the NPs were also recorded beyond 180 min from time to time to determine the ultimate stability. The effect of temperature (ambient to 100 °C) was studied at optimum pH and time conditions. Silver particles were synthesized in a similar manner by replacing $HAuCl_4 \cdot 3H_2O$ with $AgNO_3$. The change in color from colorless to yellowish brown was observed in about 60 min.

The NP suspensions thus obtained were washed several times with Nanopure® water in order to remove any unreacted gold or silver salts. The purple color remained stable for a very long time (a period of more than two years has lapsed at the time of writing this manuscript when it was last observed).

2.3.1. SPR spectroscopy

The NP suspension was appropriately diluted with water to obtain the SPR spectrum in 200–700 nm range by using Pharmaspec UV-1700 (Shimadzu, Japan) UV–Vis spectrophotometer, 1 cm quartz cell and AX suspension in Nanopure® water as the reference.

2.3.2. X-ray diffraction

The XRD spectra were recorded on Bruker D8 Discover (Germany) diffractometer using monochromatic Cu Kα radiation (λ = 1.5406 Å) operating at 40 kV and 30 mA. The data were collected over a 10–80° 2θ range by using freeze-dried NPs.

2.3.3. Atomic force microscopy

The AFM images of AX film (5.0 μm × 5.0 μm) with dispersed gold NPs were obtained by using Scanning Probe Microscope SPM-9500 J3 (Shimadzu, Japan) in the contact mode under normal

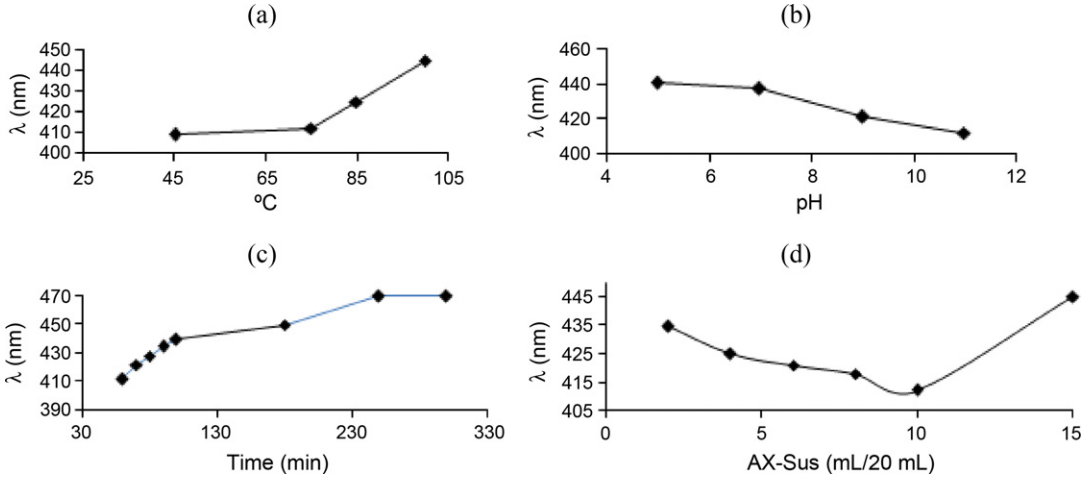

Fig. 1. Effect of (a) temperature, (b) pH, (c) time and (d) amount of AX on the SPR spectrum of S5.

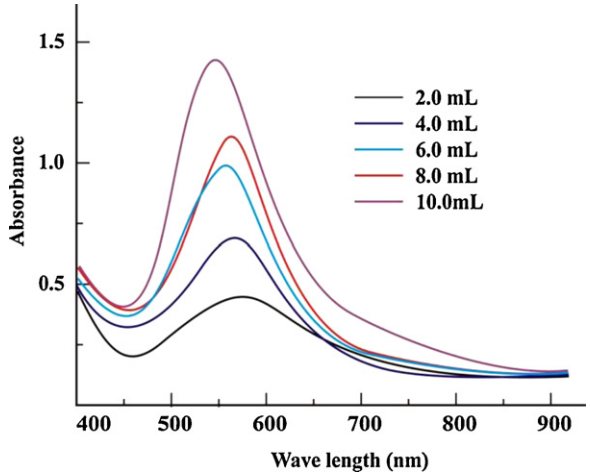

Fig. 2. SPR spectra of AuNPs with varying amounts of AX-Sus.

atmospheric conditions. A freshly prepared sample was deposited on a fine metal surface in dust-free environment for this analysis.

2.3.4. Scanning electron microscopy

Scanning electron microscopic images of selected NPs were obtained by using SEM S-3700N (Hitachi Japan) without sputter coating because the NPs were self-conducting.

2.3.5. Transmission electron microscopy

An ultrasonically dispersed sample of the solution of NPs (one drop) was placed on a carbon grid, dried at room temperature in clean environment and TEM images were obtained by using JEM-1200EX (JEOL, Japan) microscope at an accelerating voltage of 120 kV. The size distribution was determined by measuring the diameter of about 300 particles and using Origin 7.5 software, which was further confirmed by calculating the size from the highest intensity of XRD pattern by use of Debye–Scherrer equation ($D = 0.9\lambda/\beta \cos\theta$, where the symbols have their usual meaning).

3. Results and discussion

3.1. Synthesis and optimization of conditions

The gold and silver NPs were successfully synthesized by reactions of gold and silver salts with the AX isolated from ispaghula seed husk. The synthetic conditions were optimized in terms of temperature, pH, time, and concentrations of AX and metal salts with respect to SPR spectral changes. The results are shown in Figs. 1 and 2. The SPR absorbance is extremely sensitive to size and shape of particles, inter-particle distance, and the surrounding media (Kelly, Coronado, Zhao, & Schatz, 2003). Thus optimization was successfully carried out by use of SPR spectra.

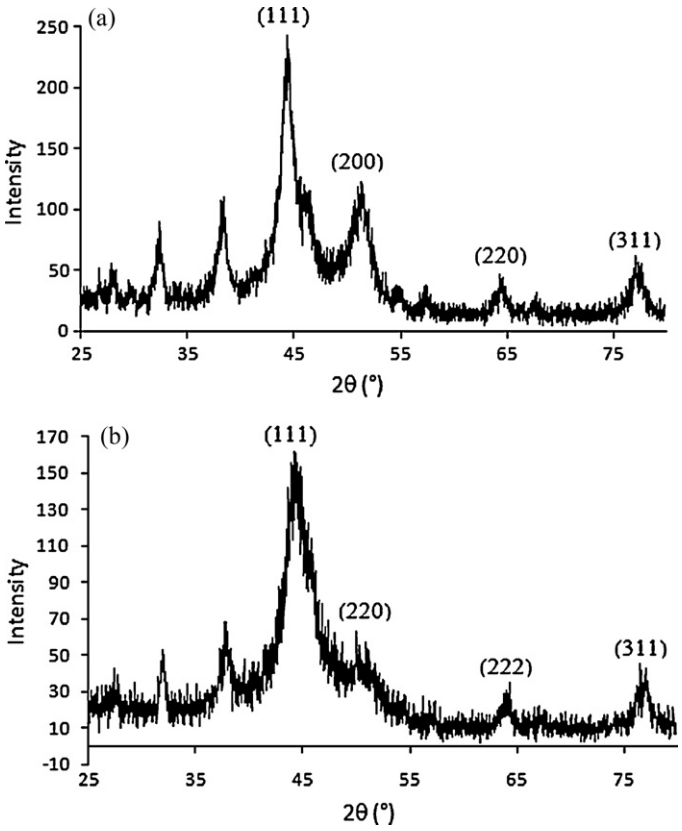

Fig. 3. XRD spectra of (a) AgNPs (S5) and (b) AuNPs (G4) dispersed in the polymer.

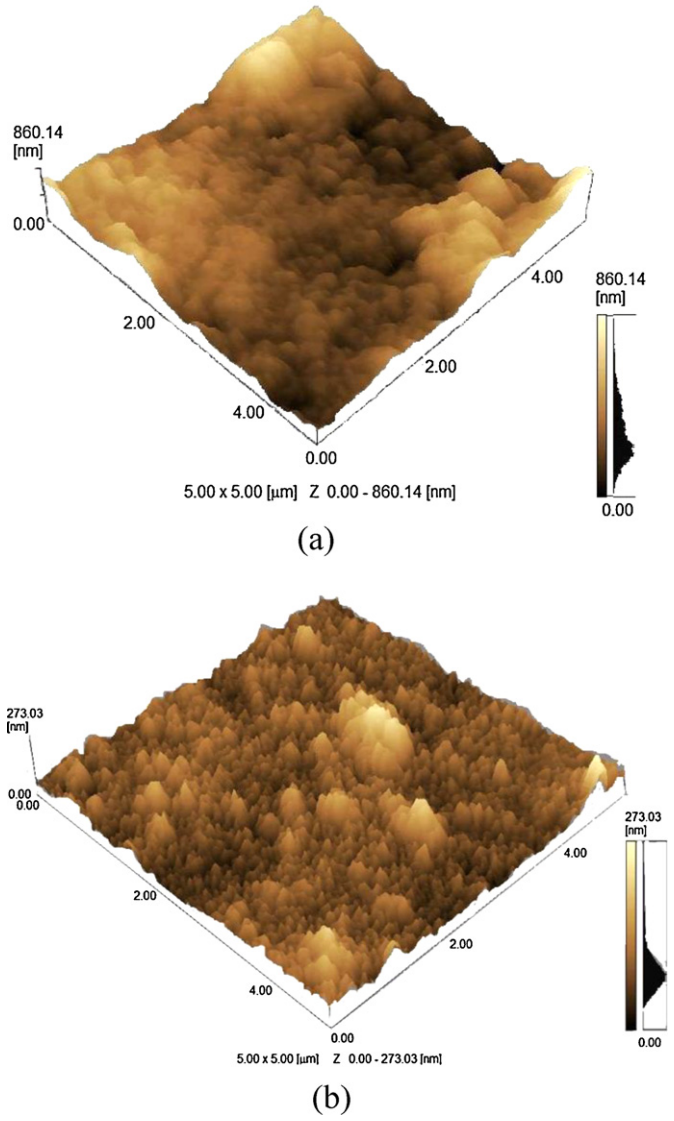

Fig. 4. AFM images of AX film (a) without and (b) with AuNPs (G4).

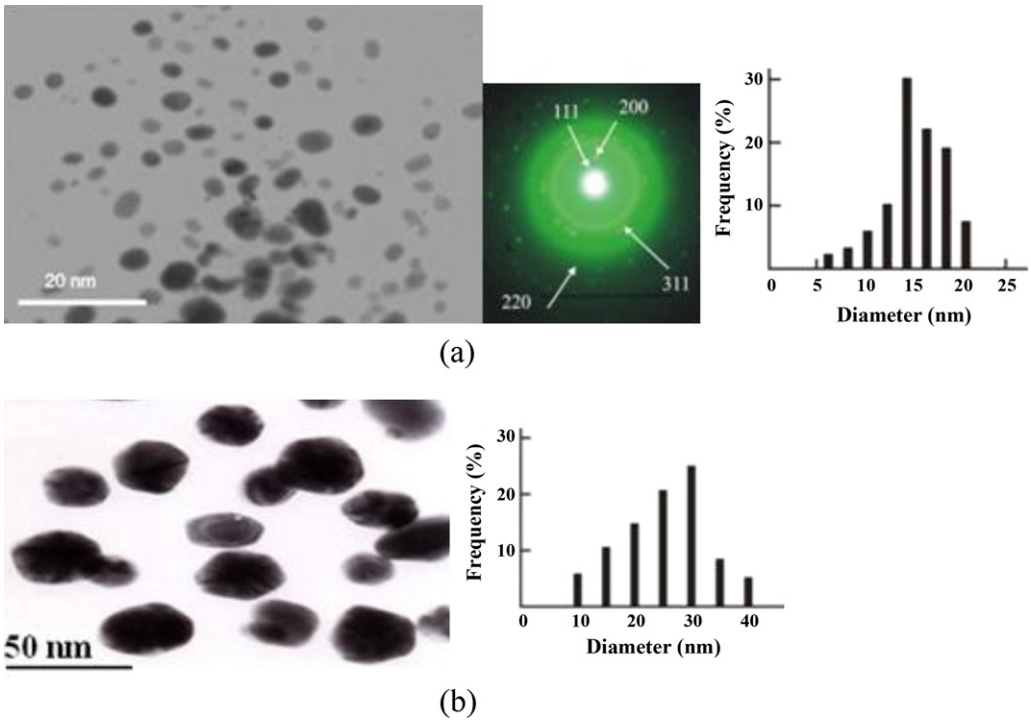

Fig. 5. TEM images and particle size distribution histograms of (a) AgNPs (S5) and (b) AuNPs (G4).

3.1.1. AgNPs

Fig. 1a shows the effect of temperature on the SPR spectrum of a sample (S5) at pH 11, time 60 min, and AX-Sus 10 mL per 20 mL. There was no SPR band observed in the spectrum of the reaction carried out at 25 °C. Beyond 25 °C up to 100 °C the absorption started coming up between 409 and 445 nm. This temperature dependent increase in the peak intensity shows that the silver ions reduction depends upon the temperature. This effect is in line with the observations by other workers (Pastoriza-Santos & Liz-Marzán, 1999; Mock, Barbic, Smith, Schultz, & Schultz, 2002). The absorption at 412 nm, corresponding to the size range of 5–12 nm (Shivaji, Madhu, & Singh, 2011), was observed at 75 °C. Similarly the optimum pH to obtain the desired absorption at 412 nm was found to be 11. At pH 4.0 no absorption maximum was observed in the range of 400–450 nm even after 24 h. However, an absorption band appeared at about 440 nm when pH was raised to 5. The size of particles formed at pH 5, however, was large which decreased with increasing pH up to 11 (Fig. 1b).

The maximum absorption at 412 nm was achieved after 60 min under optimum conditions of temperature and pH (Fig. 1c). The optimum amount of AX-Sus for 10 mL of 1.0 mM $AgNO_3$ to obtain the peak at 412 nm was found to be 10 mL (Fig. 1d). The absorption maximum moved from 435 to 412 nm as the amount of AX-Sus increased from 2.0 to 10.0 mL per 20 mL and it shifted to 445 nm at 15 mL of AX-Sus. This effect may be attributed to restricted movement of particles in the medium with increasing viscosity (Huang & Yang, 2004).

3.1.2. AuNPs

The SPR spectra of the AuNPs with varying amount of AX-Sus are shown in Fig. 2. The particles exhibited characteristic absorption maxima at 535–560 nm. Position of the absorption maximum varied with change in temperature, pH, reaction time and concentrations of the AX-Sus and the gold salt. The optimum conditions for obtaining a sharp absorption band at 535 nm, characteristic of AuNPs having size in the range 10–25 nm (Kumar et al., 2011), were determined through experimentation as described for AgNPs, and were found to be: temperature: 80 °C, pH: 6, time: 40 min, amount of AX-Sus per 20 mL: 8 mL, and amount of 1.0 mM $HAuCl_4 \cdot 3H_2O$ per 20 mL: 10 mL. With the increase in temperature from 25 °C to 80 °C, an increase in peak sharpness was observed indicating a change in particle size.

3.1.3. X-ray diffraction analysis

The XRD spectra of the synthesized AgNPs and AuNPs are shown in Fig. 3. The spectra are characteristic of face-centered cubic phase (JCPDS File No. 87-0720). The diffraction peaks can be assigned to (1 1 1), (2 0 0), (2 2 2) and (3 1 1) planes as shown on the pictures. The sizes of the particles as calculated by use of Debye–Scherrer equation were found to be 6–22 and 10–25 nm for silver and gold, respectively. The Bragg reflections (2 0 0), (2 2 0) and (3 1 1) were weak and broadened relative to the intense (1 1 1) reflection. This feature indicates that the nanocrystals are mainly oriented along (1 1 1) plane and are of smaller size as confirmed by TEM data. There were some unidentified peaks in the spectra which may be due to crystallization of an organic material from AX on the surface of the nanoparticles.

3.1.4. AFM and TEM analysis

Surface morphologies of AX films with and without nanoparticles are depicted in the AFM images (Fig. 4). It can be seen that the surface morphology changed substantially after dispersion of nanoparticles into the polymeric matrix. The TEM images of AgNPs (S5) and AuNPs (G4) along with size distribution histograms are shown in Fig. 5. Average size of AgNPs was found to be 16 nm with the range 5–20 nm. These results are consistent with the SPR and XRD data. Crystalline structure of the particles was confirmed by the SAED pattern exhibiting bright circular spots corresponding to (1 1 1), (2 0 0), (2 2 0) and (3 1 1) reflection planes. The d-spacings of the ring patterns correspond well to the XRD spectra. The TEM image of AuNPs depicted an average particle size of 20 nm with a range of 8–30 nm. This was also supported by the SPR and XRD

data. All these measurements were replicated under optimum conditions on the AX-Sus obtained from three different sources and thereby reproducibility was demonstrated.

This study clearly demonstrates that AX works as the reducing and stabilizing agent simultaneously. It may be postulated that polysaccharides hydrolyze to some extent into monosaccharides which in turn exist in cyclic and acyclic (aldehyde form) forms in equilibrium in aqueous medium (Iqbal, Khurshid, & Iqbal, 1993). Thus the aldehyde group becomes available for reduction of metal ions. However, it may be noted that AgNPs were produced in a basic and AuNPs in an acidic environment. This observation points toward different chemistries taking place with these elements, which needs to be investigated further. This study has identified AX as the excellent stabilizing agent as the AgNPs and AuNPs dispersed in it exhibited unaltered particle size after the lapse of over two years time. The AgNPs and AuNPs possessing exceptional high stability in AX-Sus can be used for various biomedical and engineering applications without the risks of contamination by conventional reducing and capping agents.

4. Conclusions

Silver and gold NPs having particle size 5–20 and 8–30 nm respectively were synthesized by use of AX, from ispaghula seed husk, as the reducing and stabilizing agent. The method used in this work totally eliminates the use of noxious reducing and stabilizing agents. The particles prepared by this method possess exceptional stability as more than two years passed when they were last observed at the time of writing this paper. As the AX used in this work is highly biocompatible, the AgNPs and AuNPs thus prepared can be safely used for various biomedical and engineering applications.

References

Akbar, J., Iqbal, M. S., Chaudhary, M. T., Yasin, T., & Massey, S. (2012). A QSPR study of drug release from an arabinoxylan using ab initio optimization and neural networks. *Carbohydrate Polymers*, *88*(4), 1348–1357.

Du, W. L., Niu, S. S., Xu, Y. L., Xu, Z. R., & Fan, C. L. (2009). Antibacterial activity of chitosan tripolyphosphate nanoparticles loaded with various metal ions. *Carbohydrate Polymers*, *75*, 385–389.

Guzmán, M. G., Dille, J., & Godet, S. (2009). Synthesis of silver nanoparticles by chemical reduction method and their antibacterial activity. *International Journal of Chemical and Biomolecular Engineering*, *2*, 104–111.

Huang, H. Z., & Yang, X. R. (2004). Synthesis of chitosan-stabilized gold nanoparticles in the absence/presence of tripolyphosphate. *Biomacromolecules*, *5*, 2340–2346.

Iqbal, M. S., Khurshid, S. J., & Iqbal, M. Z. (1993). Preparation, characterization, and biologic evaluation of copper(1I)-Schiff base complexes derived from anthranilic acid and aldoses. *Canadian Journal of Chemistry*, *71*, 629–633.

Iqbal, M. S., Akbar, J., Hussain, M. A., Saghir, S., & Sher, M. (2011). Evaluation of hot-water extracted arabinoxylans from ispaghula seeds as drug carriers. *Carbohydrate Polymers*, *83*(3), 1218–1225.

Kelly, K. L., Coronado, E., Zhao, L. L., & Schatz, C. G. (2003). The optical properties of metal nanoparticles: the influence of size, shape, and dielectric environment. *Journal of Physical Chemistry B*, *107*, 668–677.

Kora, A. J., Sashidhar, R. B., & Arunachalam, J. (2010). Gum kondagogu (*Cochlospermum gossypium*): A template for the green synthesis and stabilization of silver nanoparticles with antibacterial application. *Carbohydrate Polymers*, *82*, 670–679.

Kumar, V. G., Gokavarapu, S. D., Rajeswari, A., Dhas, T. S., Karthick, V., Kapadia, Z., et al. (2011). Facile green synthesis of gold nanoparticles using leaf extract of anti-diabetic potent *Cassia articulate*. *Colloids and Surfaces B: Biointerfaces*, *87*, 159–163.

Mock, J. J., Barbic, M., Smith, D. R., Schultz, D. A., & Schultz, S. (2002). Shape effects in plasmon resonance of individual colloidal silver nanoparticles. *Journal of Chemical Physics*, *116*, 6755–6759.

Mubarak, A. D., Thajuddin, N., Jeganathan, K., & Gunasekaran, M. (2011). Plant extract mediated synthesis of silver and gold nanoparticles and its antibacterial activity against clinically isolated pathogens. *Colloids and Surfaces B: Biointerfaces*, *85*, 360–365.

Pastoriza-Santos, I., & Liz-Marzán, L. M. (1999). Formation and stabilization of silver nanoparticles through reduction by N,N-dimethylformamide. *Langmuir*, *15*, 948–951.

Raveendran, P., Fu, J., & Wallen, S. L. (2003). Completely green synthesis and stabilization of metal nanoparticles. *Journal of the American Chemical Society*, *125*, 13940–13941.

Saghir, S., Iqbal, M. S., Hussain, M. A., Koschella, A., & Heinze, T. (2008). Structure characterization and carboxymethylation of arabinoxylan isolated from ispaghula (*plantago ovata*) seed husk. *Carbohydrate Polymers*, *74*, 309–317.

Shivaji, S., Madhu, S., & Singh, S. (2011). Extracellular synthesis of antibacterial silver nanoparticles using psychrophilic bacteria. *Process Biochemistry*, *46*, 1800–1807.

Sun, Y., & Xia, Y. (2003). Gold and silver nanoparticles: A class of chromophores with colors tunable in the range from 400 to 750 nm. *Analyst*, *128*, 686–691.

Van Hyning, D. L., & Zukoski, C. F. (1998). Formation mechanisms and aggregation behavior of borohydride reduced silver particles. *Langmuir*, *14*, 7034–7046.

Yan, W., Wang, R., Xu, Z., Xu, J., Lin, L., Shen, Z., et al. (2006). A novel, practical and green synthesis of Ag nanoparticles catalyst and its application in three-component coupling of aldehyde alkyne, and amine. *Journal of Molecular Catalysis A: Chemical*, *255*, 81–85.

You, C.-C., Chompoosor, A., & Rotello, V. M. (2007). The biomacromolecule–nanoparticle interface. *Nanotoday*, *2*, 34–43.